Cell Cycle 13:14, 2248–2261; July 15, 2014; © 2014 Landes Bioscience

Spatial regulation of Aurora A activity during mitotic spindle assembly requires RHAMM to correctly localize TPX2

Helen Chen[1], Pooja Mohan[1], Jihong Jiang[1], Oksana Nemirovsky[1], Daniel He[1], Markus C Fleisch[2], Dieter Niederacher[2], Linda M Pilarski[3], C James Lim[1], and Christopher A Maxwell[1,*]

[1]Department of Pediatrics; Child and Family Research Institute; University of British Columbia; Vancouver, British Columbia, Canada; [2]Department of Gynaecology and Obstetrics; University Hospital Düsseldorf; Heinrich-Heine University; Düsseldorf, Germany; [3]Department of Oncology; University of Alberta and Cross Cancer Institute; Edmonton, Alberta, Canada

Keywords: Aurora kinase A, mitosis, RHAMM, spindle assembly, TPX2

Construction of a mitotic spindle requires biochemical pathways to assemble spindle microtubules and structural proteins to organize these microtubules into a bipolar array. Through a complex with dynein, the receptor for hyaluronan-mediated motility (RHAMM) cross-links mitotic microtubules to provide structural support, maintain spindle integrity, and correctly orient the mitotic spindle. Here, we locate RHAMM to sites of microtubule assembly at centrosomes and non-centrosome sites near kinetochores and demonstrate that RHAMM is required for the activation of Aurora kinase A. Silencing of RHAMM delays the kinetics of spindle assembly, mislocalizes targeting protein for XKlp2 (TPX2), and attenuates the localized activation of Aurora kinase A with a consequent reduction in mitotic spindle length. The RHAMM–TPX2 complex requires a C-terminal basic leucine zipper in RHAMM and a domain that includes the nuclear localization signal in TPX2. Together, our findings identify RHAMM as a critical regulator for Aurora kinase A signaling and suggest that RHAMM ensures bipolar spindle assembly and mitotic progression through the integration of biochemical and structural pathways.

Introduction

Cell division relies upon the assembly of a microtubule-based mitotic spindle apparatus that captures, aligns, and segregates duplicated chromosomes. This construction process requires biochemical signaling to promote microtubule assembly and subsequent structural cues to organize these microtubules into a bipolar array. The major sites for microtubule assembly are the centrosomes, which form the spindle poles, but assembly also occurs near kinetochores.[1] Microtubule assembly is spatially regulated by localized activation of the mitotic kinase, Aurora A.[2-5] These microtubules are then organized into a bipolar structure through the actions of protein complexes that include molecular motors, such as dyneins and kinesins.

The receptor for hyaluronan-mediated motility (RHAMM) is a microtubule-associated protein that ensures the structural integrity of the mitotic spindle. RHAMM is able to bind microtubules directly at the amino (N) terminus and indirectly at the carbox (C) terminus through a complex with dynein. In this way, RHAMM serves as a structural adaptor that cross links microtubules.[6-8] RHAMM is also part of a heterodimer docking complex that links dynein to the mitotic spindle, which functions to define spindle orientation during metaphase.[9] Moreover, XRHAMM, the *Xenopus* ortholog of human RHAMM, focuses anastral spindle microtubules, and this action relies upon a C-terminal basic leucine zipper (bZIP) motif.[10,11] Thus, to date, RHAMM is known to play key structural roles at the mitotic spindle.

The C-terminal bZIP motif in RHAMM is 70% homologous with the C terminus of *Xenopus* kinesin-like protein 2 (XKlp2).[6] This domain in XKlp2 is necessary for a complex with dynein and the spindle assembly factor, targeting protein for XKlp2 (TPX2).[12] In both human and *Xenopus* mitotic cells, RHAMM is a partner protein of TPX2; a ternary complex between these 2 proteins and dynein maintains spindle integrity and promotes spindle pole focusing.[6,10] TPX2 is also a co-factor for Aurora A and is both sufficient to activate the kinase above basal levels and necessary for optimal kinase activity.[13,14] As 40–60% of TPX2 is in a complex with RHAMM in human mitotic cells,[7] a regulatory relationship between RHAMM and Aurora A activity has been postulated[10,11,15] but not yet been demonstrated.

Aurora A promotes microtubule assembly by targeting its substrates to sites of assembly[2-5,16,17] and by protecting these substrates from proteolytic degradation.[15,18,19] Aurora A is under regulatory control by multiple factors,[13,20-22] but a complex between

*Correspondence to: Chris Maxwell; Email: cmaxwell@cfri.ca
Submitted: 04/11/2014; Accepted: 05/17/2014; Published Online: 05/29/2014
http://dx.doi.org/10.4161/cc.29270

Aurora A and TPX2 is necessary for optimal kinase activity.[13,14,23] Indeed, microtubule assembly near to the kinetochores relies on the localized activation of Aurora A by TPX2, which is released from binding partners in response to a gradient of active Ran on the chromosomes.[1,16,24,25] Thus, Aurora A activity is dependent on and limited by TPX2 availability and location, which may be regulated by RHAMM.

Here, we found that RHAMM localized to the centrosomes and near to the kinetochores, and promoted microtubule assembly at these sites. The silencing of RHAMM mislocalized TPX2 and attenuated both the kinetics of mitotic spindle assembly and mitotic microtubule regrowth. As a result, the activity of Aurora A was attenuated, and mitotic spindle length was reduced. Overall, our findings demonstrate a novel role for RHAMM in the regulation of Aurora A activity and suggest that RHAMM integrates structural and biochemical pathways to ensure proper mitotic spindle assembly and organization.

Results

RHAMM localized to centrosome and non-centrosomal spindle microtubule assembly sites

To query a putative role for RHAMM during spindle assembly, we used immunofluorescence to localize RHAMM in prophase cells and found that it co-localized with a centrosome marker (gamma-tubulin, TUBG1) and decorated mitotic microtubules and spindle poles in cells at later stages of mitosis (**Fig. 1A**) (**Fig. S1A**).[6] In prophase HeLa cells, we localized RHAMM to discrete foci within the chromosome volumes (**Fig. 1A**). Ectopically expressed GFP-RHAMM also localized to punctuate, non-centrosomal sites, which co-localized near to a kinetochore marker (Bub1-related kinase, BubR1) (**Fig. 1A**). This localization was more pronounced in the hematopoietic cell line, RPMI-8226 (**Fig. 1B,** arrows). We asked whether these foci may be sites for microtubule assembly using a regrowth assay in which microtubules in mitotic cells were depolymerized with nocodazole and allowed to regrow during a recovery phase. As shown at 2 m for recovery, microtubules (β-tubulin, TUBB) were first assembled at centrosomes, demarked by TUBG1 (**Fig. 1C**). By 6 min for recovery, mitotic microtubules were assembled at centrosomes as well as non-centrosome sites, which co-localized with BubR1 (**Fig. 1C**). In these microtubule-regrowth experiments in mitotic cells, RHAMM localized to both centrosome and non-centrosome sites of microtubule assembly (**Fig. 1C**).

RHAMM is required for normal mitotic spindle assembly kinetics and architecture

To query whether RHAMM contributes to microtubule assembly or is simply a passenger microtubule-associated protein at these sites, cells were separately treated with 3 siRNA duplexes that target the untranslated regions (UTRs) of RHAMM mRNA, which enabled us to silence RHAMM and rescue function through transient expression of the wild-type transgene tagged with GFP at the vN-terminus (GFP-RHAMM). With the outlined protocol (**Fig. S1B**), endogenous RHAMM mRNA levels were reduced by 40–70% (**Fig. S1C**), which translated to a 70–80% reduction in the levels of RHAMM protein (**Fig. 1D**). Rescue with GFP-RHAMM resulted in transgene expression at levels that approximated endogenous RHAMM levels (top band is GFP-RHAMM in **Fig. 1E**), and we confirmed that GFP-RHAMM localized in a manner that is similar to that of the endogenous protein (**Fig. S1D**). Consistent with the previously established role for RHAMM as a structural mitotic spindle protein, the silencing of RHAMM resulted in a significant increase in both the proportion of cells with mitotic spindle defects, such as multipolar spindles and disorganized spindles (**Fig. 1F**) and multinucleated cells (**Fig. 1G**), which may result through the failure of cell division. Importantly, both of these depletion phenotypes could be rescued through the transient expression of GFP-RHAMM (**Fig. 1F and G**). Moreover, in RHAMM-silenced HeLa cells, we found a significant increase in the proportion of mitotic cells, which suggested that the silencing of RHAMM induced a mitotic arrest and/or delayed mitotic kinetics (**Fig. 1H**).

To help distinguish between mitotic arrest and delayed kinetics, living, non-synchronized HeLa cells were followed by time-lapse microscopy as they transited through mitosis (**Fig. 2A and B**; **Videos S1–4**). We quantified the time necessary for spindle assembly and mitosis completion by tracking the progression of mitotic cells (**Fig. 2C**). Spindle assembly duration was defined as the time from the onset of prophase (chromosome condensation) to the onset of metaphase (chromosome alignment), and mitosis duration was measured from the onset of prophase to the end of telophase (disappearance of the midzone spindle). In cells pretreated with scrambled control siRNA, the average duration for spindle assembly was 26 ± 9 min, and these cells completed mitosis in 106 ± 17 min (**Fig. 2C**; **Video S1**), which are similar kinetics to those of untreated cells (27 ± 13 min and 118 ± 24 min, respectively). Silencing of RHAMM, however, resulted in a significant delay in both the time necessary to assemble a bipolar spindle and the time necessary to complete mitosis (51 ± 17 min and 185 ± 32 min, respectively) (**Fig. 2C**; **Videos S2 and 3**); indeed, 43% of mitotic cells pretreated with siRNA duplexes targeting RHAMM were unable to complete mitosis during the imaging time, and these cells were excluded from the quantitation of kinetics (**Fig. 2C**). Moreover, we found that phenotypically normal mitotic spindles would rotate freely in cells pretreated with siRNA targeting RHAMM (**Video S3**), consistent with a necessary role for RHAMM in the establishment of mitotic spindle orientation.[9] Mitotic defects that accompanied the silencing of RHAMM were attenuated when GFP-RHAMM was transiently expressed (**Fig. 2B and C**; **Video S4**), which indicates that defects in spindle assembly, both kinetics and structure, can be assigned to the specific loss of RHAMM.

RHAMM is required for TPX2 localization and stability

To dissect the contributions of RHAMM to mitotic spindle assembly, the kinetics of mitotic microtubule regrowth after nocodazole depolymerization were followed in prophase cells that were previously treated with a scrambled control siRNA duplex or with duplexes targeting RHAMM. In comparison to control-treated cells, the silencing of RHAMM delayed the assembly of microtubule asters and the formation of a bipolar spindle

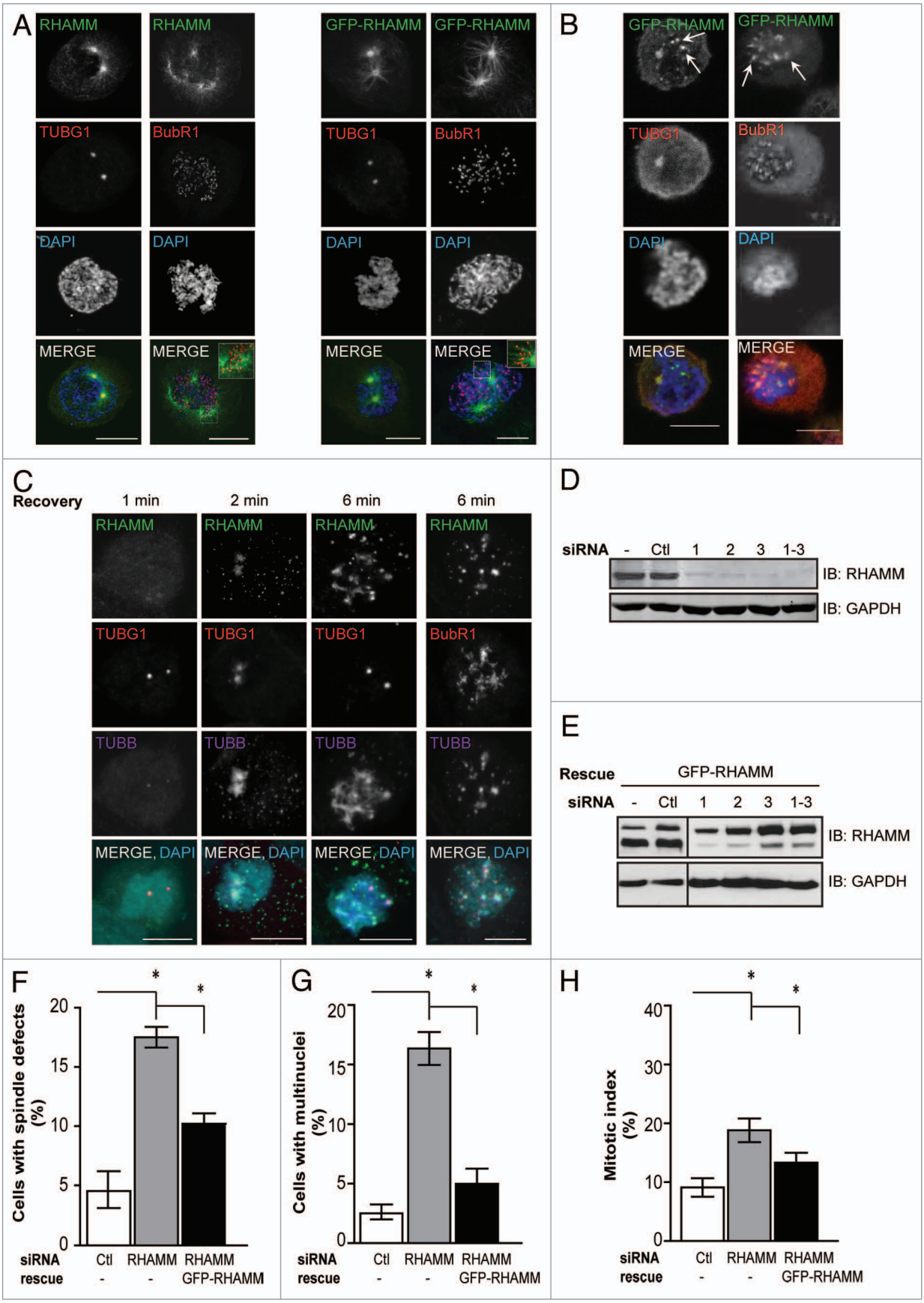

Figure 1. For figure legend, see page 2251.

Figure 1 (See previous page). RHAMM participates in spindle microtubule assembly at both centrosomal and non-centrosomal sites during early mitosis and is required for proper spindle architecture and mitosis kinetics. (**A**) In prophase HeLa cells, RHAMM was located at the centrosomes (identified by gamma-tubulin, TUBG1) as well as non-centrosomal sites near kinetochores (identified by BubR1) within nuclear volumes (identified by DAPI) as determined for endogenous RHAMM by immunofluorescence and by the expression of exogenous GFP-RHAMM. Scale bars = 10 μm. (**B**) In prophase RPMI 8226 cells, exogenous GFP-RHAMM colocalized with TUBG1 at the centrosomes and BubR1 at the kinetochores within nuclear volumes. Scale bars = 10 μm. (**C**) In mitotic HeLa cells, RHAMM localization at spindle microtubule assembly sites was tracked at indicated times following depolymerization by nocodazole. Microtubule assembly (identified by β-tubulin, TUBB) initiated at 2 min around the centrosomes (TUBG1) and included non-centrosomal sites near the kinetochores (BubR1) by 6 min. RHAMM was located at both centrosomes and non-centrosomal spindle microtubule assembly sites. Scale bars = 10 μm. (**D**) HeLa cells were treated with scrambled control (Ctl) siRNA or siRNA duplexes targeting the 3′ UTR (#1, #2) or the 5′ UTR (#3) of RHAMM mRNA as well as pooled siRNA (1–3) to deplete endogenous RHAMM. RHAMM expression was measured by western blot analysis 48–72 h following transfection. Equal loading was confirmed with GAPDH. (**E**) Exogenous GFP-RHAMM was transfected into cells 48 h after siRNA transfection. After a further 48 h, the expression of RHAMM, and GFP-RHAMM (shifted by 27 kD), were measured by western blot analysis. GFP-RHAMM was expressed in RHAMM-silenced cells at a level similar to that of endogenous RHAMM. Equal loading was confirmed with GAPDH. (**F**) Aberrant spindle figures (multipolar spindle, disorganized spindle and unattached chromosomes) were significantly more frequent in RHAMM-silenced cells. Rescue with GFP-RHAMM was sufficient to reduce these aberrant phenotypes. (mean ± s.d., n = 3, $*P < 0.05$). (**G**) Multinucleated cells were significantly more frequent in RHAMM-silenced cells. Rescue with GFP-RHAMM was sufficient to reduce these aberrant phenotypes. (mean ± s.d., n = 3, $*P < 0.05$). (**H**) Mitotic indices were determined by DAPI staining in immunofluorescence. The mitotic index was significantly higher in RHAMM-silenced cells. Rescue with GFP-RHAMM was sufficient to reduce the mitotic index. (mean ± s.d., n = 3, $*P < 0.05$)

following nocodazole washout (**Fig. 3A**; **Videos S5 and 6**), suggesting that RHAMM may play a role in seeding or establishing microtubule assembly sites. The attenuation of assembly was quantified in fixed cells at 6 min following recovery, when both centrosome and non-centrosomal assembly sites were present in the control-treated cells. Silencing of RHAMM resulted in a significant reduction in the number of microtubule foci assembled at non-centrosomal sites, and rescue with GFP-RHAMM was sufficient to recover non-centrosome microtubule assembly in RHAMM-silenced mitotic cells (**Fig. 3B**).

In *Xenopus* meiotic cell extracts, immunodepletion of XRHAMM prevented TPX2 concentration to DMSO-induced microtubule spindle poles,[10] so we examined whether the silencing of RHAMM in mitotic HeLa cells prevented the localization of TPX2 to sites of microtubule assembly. In RHAMM-silenced mitotic cells, we found significantly fewer TPX2-positive microtubule regrowth sites (**Fig. 3C**). Pre-treatment of mitotic cells with nocodazole may dramatically alter microtubule assembly kinetics due, in part, to residual drug. So, we examined the immunolocalization of TPX2 in non-synchronized mitotic HeLa cells and found that TPX2 was lost from spindle poles (i.e., regions of interest identified by TUBG1) in RHAMM-silenced mitotic cells (**Fig. 3D**).

In both of the described assays, the abundance of TPX2 appeared reduced by immunofluorescence in RHAMM-silenced cells. To test the possibility that the specific loss of RHAMM altered the stability of TPX2, the abundance of these proteins were determined in lysates from G_2/M synchronized cell populations, as each gene product is strongly cell cycle regulated.[6,7,26] Synchronized populations of RHAMM-silenced cells showed reduced abundance of RHAMM and TPX2, but not the GTP binding protein Ran (**Fig. 3E**). Pre-treatment of cells with the proteasome inhibitor MG132 was sufficient to recover the level of TPX2 in RHAMM-silenced cells (**Fig. 3E**), which implies that the loss of RHAMM augments proteasome-dependent turnover of TPX2.

We next measured the levels of Aurora A and active, autophosphorylated Aurora A (pAurora A) in these lysates. Like TPX2, the abundance of Aurora A and the levels of pAurora A were reduced in RHAMM-silenced G_2/M synchronized cell lysates (**Fig. 3F**). Proteasome inhibition was sufficient to recover the total level of Aurora A (**Fig. 3F**). However, proteasome inhibition did not completely recover pAurora A, which remained attenuated in the presence of the correct levels of total Aurora A and TPX2 (**Fig. 3F**). These data support a regulatory role for RHAMM in the activation of Aurora A. The silencing of RHAMM reduced the abundance of TPX2, but even when the abundance of TPX2 was restored through proteasome inhibition, the level of active pAurora A was sub-optimal due to the mislocalization of TPX2.

The C-terminal bZIP of RHAMM binds near the nuclear localization signal of TPX2 to correctly locate TPX2 to sites of microtubule assembly and control spindle length

To better define the RHAMM-TPX2 protein complex and map the domains necessary for this interaction, truncation mutants were constructed for the C-terminus of RHAMM (**Fig. 4A**). These variants for GFP-RHAMM were transiently expressed in cells depleted of endogenous RHAMM, and the ability of these variants to co-precipitate TPX2 was tested through immunoprecipitation with antibodies to GFP, or IgG control antibodies. TPX2 was efficiently co-precipitated by RHAMM variants that contained a minimal necessary binding domain of amino acids 623–679 (i.e., full-length, 1–679, and 623–724), which contains the bZIP motif (**Fig. 4B**). Indeed, mutation to arginines of the 3 leucines in the motif was sufficient to abolish TPX2 from the precipitates (**Fig. 4B**).

Reciprocal studies were performed with transient expression of truncation variants for human TPX2. Since there are essential protein-binding domains in both the N- and C terminus of TPX2, we designed various truncation mutants from wild-type transgene tagged with either mCherry at the N terminus (mCherry-TPX2) or GFP at the C terminus (TPX2-GFP) to map the domains necessary for RHAMM interaction. mCherry–TPX2 and TPX2–GFP truncation mutants were transiently expressed in HeLa cells (**Fig. 4C**) and immunoprecipitated with antibodies to GFP, antibodies to mCherry, or IgG control antibodies. mCherry-TPX2 (FL) co-precipitated RHAMM and Aurora A, which was included as a positive control (**Fig. 4D**). The Klp2-targeting domain (aa 319–783[27]) was not sufficient to

co-precipitate RHAMM (**Fig. 4D**). The N terminus of TPX2 (aa 1–319), however, was sufficient, and the deletion of the Aurora A binding domain (aa 1–40[13,27]) did not alter the complex formation (**Fig. 4D**). Together, these data localize the RHAMM-binding domain in TPX2 to amino acids 40–319, which contain an importin-α binding motif.[28]

Compressed mitotic spindles result directly from the loss of TPX2 at the pole, which attenuates kinetochore-mediated microtubule assembly and spindle length.[29,30] So, we measured TPX2 localization at spindle poles (**Fig. 5A**) and mitotic spindle length (**Fig. 5B**) to map the minimal necessary domain in RHAMM for TPX2 targeting and retention. Our observations, and findings by others[9] demonstrate that mitotic spindle orientation is disturbed in RHAMM-silenced cells. Spindle rotation may result in normal length spindles appearing compressed when viewed along the *z*-axis. To avoid this potential confounding factor, we measured pole-to-pole distance along a plane that is perpendicular to the aligned chromosomes in a 3D image, using TUBG1 as a marker protein for spindle poles.

In RHAMM-silenced cells rescued with GFP-RHAMM (full-length) or GFP-RHAMM(1–679) variants, TPX2 localized to the poles and decorated phenotypically normal mitotic

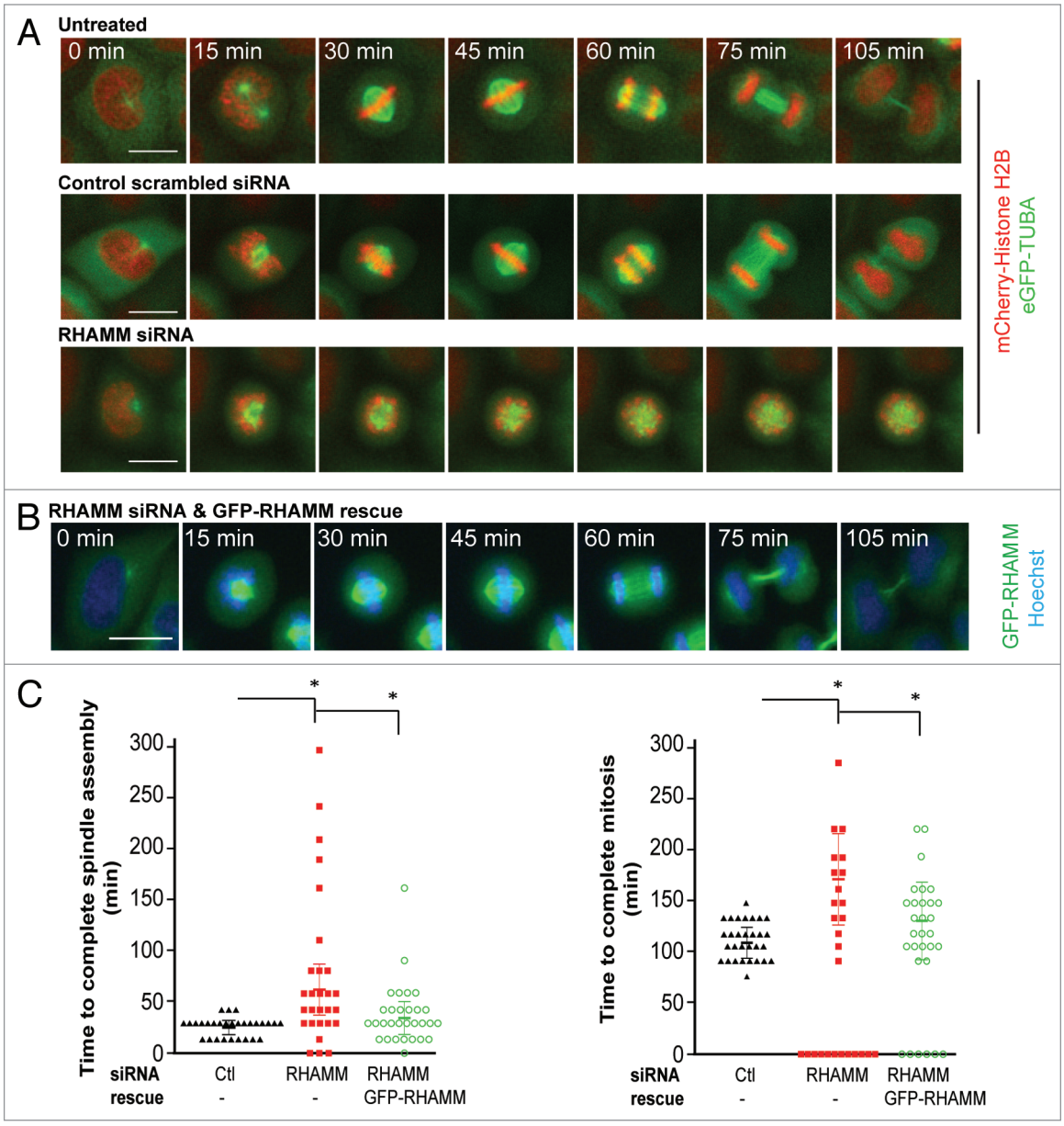

Figure 2. Proper mitotic kinetics and spindle microtubule assembly are dependent on RHAMM expression. (**A**) Living HeLa cells expressing eGFP-tubulin and mCherry Histone-H2B were treated with either control siRNA or siRNA duplexes targeting RHAMM and followed through mitosis using time-lapse microscopy. Scale bars = 10 μm. (**B**) HeLa cells were treated with siRNA duplexes targeting RHAMM and rescued with exogenous GFP-RHAMM. Cells were labeled with Hoechst to visualize DNA and followed through mitosis using time-lapse microscopy. Scale bars = 10 μm. (**C**) The kinetics for mitosis in RHAMM-silenced cells was delayed. Expression of exogenous GFP-RHAMM significantly reduced the time to transit through mitosis. Cells that did not complete mitosis during imaging are plotted at 0 min and were not included in the quantitation of mitosis duration. (mean ± s.d., n = 6, $^*P < 0.05$).

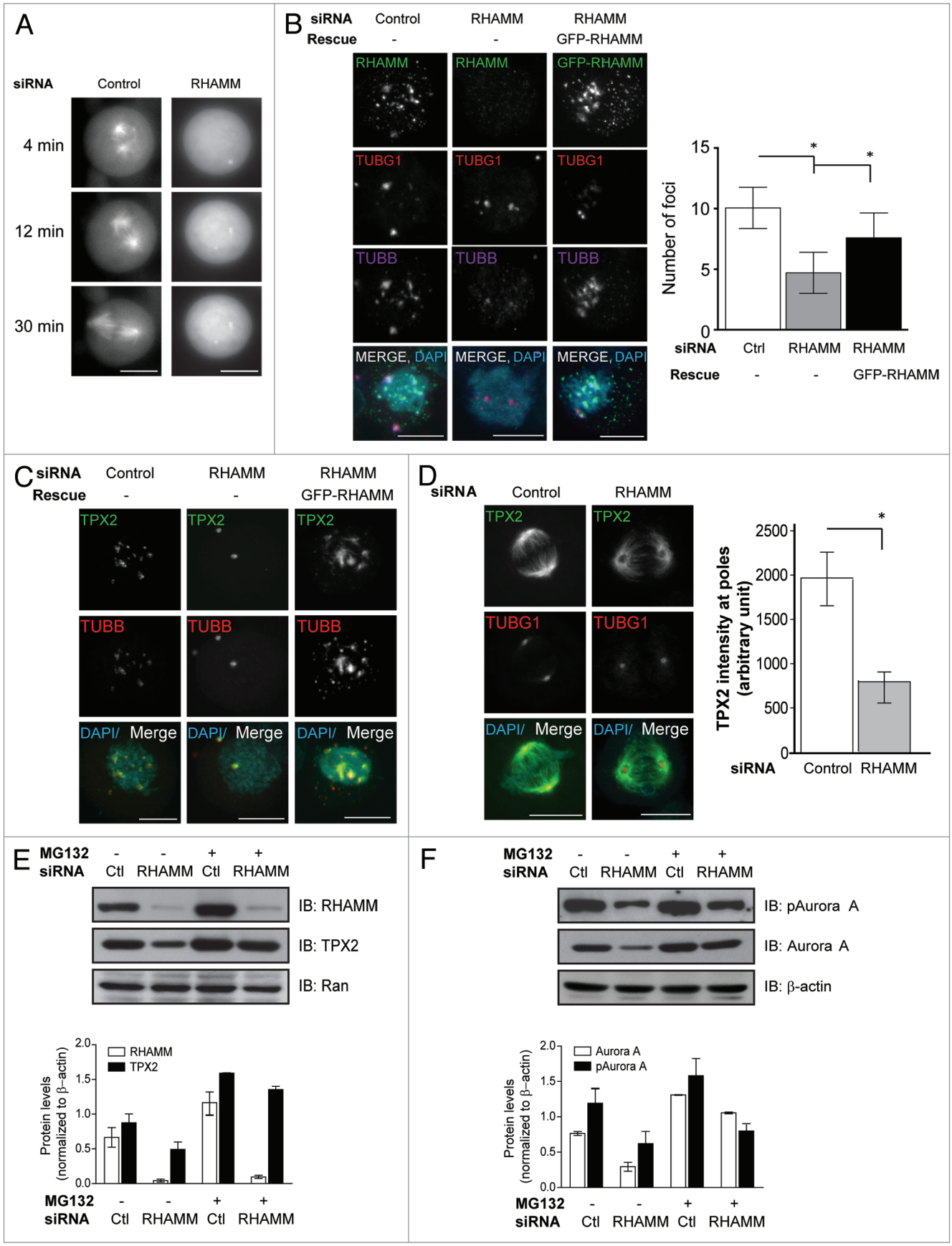

Figure 3. For figure legend, see page 2254.

Figure 3 (See previous page). RHAMM is required for spindle microtubule assembly and TPX2 localization and stability. (**A**) In living HeLa cells expressing GFP-tubulin, microtubule assembly and the formation of a bipolar spindle following nocodazole treatment was disrupted in cells treated with siRNA targeting RHAMM. Scale bars = 10 μm. (**B**) In mitotic HeLa cells recovering from nocodazole treatment, microtubule assembly at non-centrosomal sites was attenuated in RHAMM-silenced cells, and the expression of GFP-RHAMM was sufficient to re-establish microtubule assembly at these sites. Scale bars = 10 μm. (mean ± s.d., n = 4, *$P < 0.05$). (**C**) TPX2 localization to non-centrosomal microtubule assembly sites was abolished in RHAMM-silenced mitotic cells during recovery from nocodazole, and the expression of GFP-RHAMM was sufficient to re-establish microtubule assembly at these sites. Scale bars = 10 μm. (**D**) TPX2 specific immuno-staining at spindle poles (regions of interest identified by TUBG1) was significantly reduced in cells treated with siRNA targeting RHAMM. Scale bars = 10 μm. (mean ± s.d., n = 3, *$P < 0.05$). (**E**) In synchronized early mitotic cells, the levels of RHAMM and TPX2 were reduced in cells pretreated with siRNA targeting RHAMM compared with those treated with scrambled control siRNA. Proteasome inhibition (MG132, 15 μM) was sufficient to recover the level of TPX2 in RHAMM-silenced cells. Ran served as a related protein that was unaffected in RHAMM-silenced cells. Protein expression levels in immunoblotting experiments are quantified by normalizing to β-actin levels. (**F**) In synchronized early mitotic cell, the levels of Aurora A and pAurora A were reduced in cells pretreated with siRNA targeting RHAMM compared with those treated with scrambled control siRNA. Proteasome inhibition (MG132, 15 μM) was sufficient to recover the level of Aurora A, but not pAurora A, in RHAMM-silenced cells. β-actin levels confirmed equal loading. Protein expression levels in immunoblotting experiments are quantified by normalizing to β-actin levels.

spindles (**Fig. 5A**) of typical lengths (**Fig. 5B**). However, the expression of GFP-RHAMM(1–623), which lacks the bZIP motif, or GFP-RHAMM(623–724) was not sufficient to correctly localize TPX2, and, consistently, mitotic spindle lengths were significantly compressed when compared with those in control-treated cells or cells expressing full-length or GFP-RHAMM(1–679) variants (**Fig. 5B**). Thus, the bZIP motif in RHAMM is required, but is not sufficient, for the correct targeting and retention of TPX2 at spindle poles.

To define the necessary domains in TPX2 that may target RHAMM, reciprocal targeting experiments were performed in HeLa cells treated with shRNA targeting TPX2 (**Fig. S2A**). We found that RHAMM remain localized to unfocused spindle poles in TPX2-silenced mitotic cells (**Fig. 5C**). However, we observed compressed spindles in TPX2-silenced cells, in a fashion similar to RHAMM-silenced mitotic cells. These compressed phenotypes were rescued only by the expression of full-length mCherry-TPX2 and not by truncation variants (**Fig. 5D and E**). Thus, TPX2 is not required for the correct targeting and retention of RHAMM at spindle poles.

RHAMM is required for the temporally and spatially regulated activity of Aurora A

A regulatory relationship between RHAMM and Aurora A activity during mitotic spindle assembly is implied from our prior results (**Fig. 3F**) but not yet demonstrated. Therefore, we designed a series of experiments to examine the effects of RHAMM depletion on the activity of Aurora A. In asynchronous mitotic cells, we measured by immunofluorescence the levels of pAurora A at mitotic spindle poles, as demarked by TUBG1 (**Fig. 6A**); as a control for these studies, mitotic cells were pretreated with an Aurora A-specific small-molecule inhibitor, MLN8237, or vehicle DMSO control (**Fig. S2C**). Depletion of RHAMM, or pre-treatment with MLN8237, significantly reduced the levels of pAurora A at spindle poles (**Figs. 6A**; **Fig. S2C**). For kinetic and spatial analysis of Aurora A activity at non-centrosome sites of assembly, we used mitotic microtubule regrowth experiments. First, we measured pAurora A abundance by immunofluorescence at sites for microtubule regrowth following 6 min for recovery. In scrambled siRNA-treated (control) cells, or vehicle-treated cells, non-centrosome sites for assembly were strongly positive for pAurora A (**Figs. 6B**; **Fig. S2D**). Depletion of RHAMM, or pre-treatment with MLN8237, reduced pAurora A intensity at these sites (**Figs. 6B**; **Fig. S2D**).

Non-centrosome sites of assembly following recovery from nocodazole were attenuated with RHAMM depletion, which hindered the measurement of pAurora A at these sites. Thus, we utilized a FRET-based probe for Polo-like kinase 1 (PLK1) activity that is targeted to kinetochores[31] to indirectly measure the spatial and temporal activity of Aurora A. PLK1 is a substrate for Aurora A and depletion of Aurora A by siRNA was sufficient to attenuate PLK1 activity.[32-35] Following nocodazole washout, PLK1 activity is high in prometaphase cells and resolves with lower phosphorylation at metaphase alignment; the current iteration of the probe[31] tracks these kinase dynamics with an increasing FRET ratio (reflecting a decreasing level of phosphorylated substrate) as the cell progresses towards metaphase (**Fig. 6C**). We confirmed that the FRET emission ratio of the sensor was increased in the presence of the PLK1-specific inhibitor, BI2536, within prometaphase cells (**Fig. 6D**). In metaphase cells, however, PLK1 inhibition did not further augment the emission ratio, indicating, as expected, a low level of kinase activity within cells at this stage of mitosis (**Fig. 6D**). Incubation with the Aurora A-specific inhibitor, MLN8237, was sufficient to augment the emission ratio in prometaphase cells as was the pre-treatment of cells with siRNA to RHAMM, but not scrambled siRNA controls (**Fig. 6D**). Together, these data suggest that the loss of RHAMM attenuates Aurora A activity at kinetochores and sites of microtubule assembly in prometaphase cells.

Discussion

Construction of the mitotic spindle is a multi-step process that relies on microtubule assembly at various sites within the cell. RHAMM is a key cell division gene product[36] that provides structural cues to maintain spindle integrity[6,7] and establish spindle position.[9] A series of papers from work in *Xenopus* cells suggest that XRHAMM supports anastral microtubule assembly,[10,11,37] potentially through regulation of Aurora A activity. These papers attempt to mechanistically bridge the actions of the tumor-suppressive BRCA1–BARD1 complex, which targets RHAMM for degradation,[11,15] to the oncogenic Aurora A–TPX2 complex during mitotic spindle assembly. However, it is not yet clear whether XRHAMM promotes[10] or prevents[11] TPX2 availability at sites of assembly. Moreover, recent work by Barr and colleagues did not detect RHAMM (aka HMMR) at the

kinetochores and found that its depletion had no effect on cold-stable kinetochore fibers.[9] Therefore, fundamental questions remain in the literature regarding the putative contribution of RHAMM to mitotic spindle assembly, TPX2 location, and biochemical signaling through Aurora A.

Aurora A has been regarded as an important regulator for cell cycle control and mitotic progression since its initial discovery in *Drosophila*.[38] Accordingly, kinase activation is tightly regulated temporally and spatially by its cofactors. During G_2, Aurora A is activated by the LIM protein Ajuba, along with Bora and PLK1 at the centrosome to promote centrosome maturation and mitotic entry.[21,22,33] TPX2 is the most prominent coactivator of Aurora A during mitosis.[13,14,23] Thus, the regulation of spatial availability of TPX2 determines local Aurora A activity and promotes mitotic spindle assembly. Here, we identify RHAMM as a new and central regulator for Aurora A activity through the modulation of TPX2 abundance and localization.

Our studies located RHAMM to sites of microtubule assembly near kinetochores in asynchronous prophase cells and during microtubule regrowth assays in mitotic cells. This localization for RHAMM was transient in asynchronous cells, and more pronounced when GFP-RHAMM was overexpressed, but restricted to mitotic stages prior to chromosome alignment. This may explain why RHAMM was not robustly immunolocalized to cold-stable kinetochore fibers in metaphase cells.[9] Our findings that RHAMM located near kinetochores are consistent with those from studies of anastral assembly in *Xenopus* cells[10,11] and may help to interpret the findings for mitotic phenotypes linked to RHAMM depletion in a recent genome-wide screen.[36] Blind alignment of mitotic phenotypes that resulted from RHAMM depletion against all

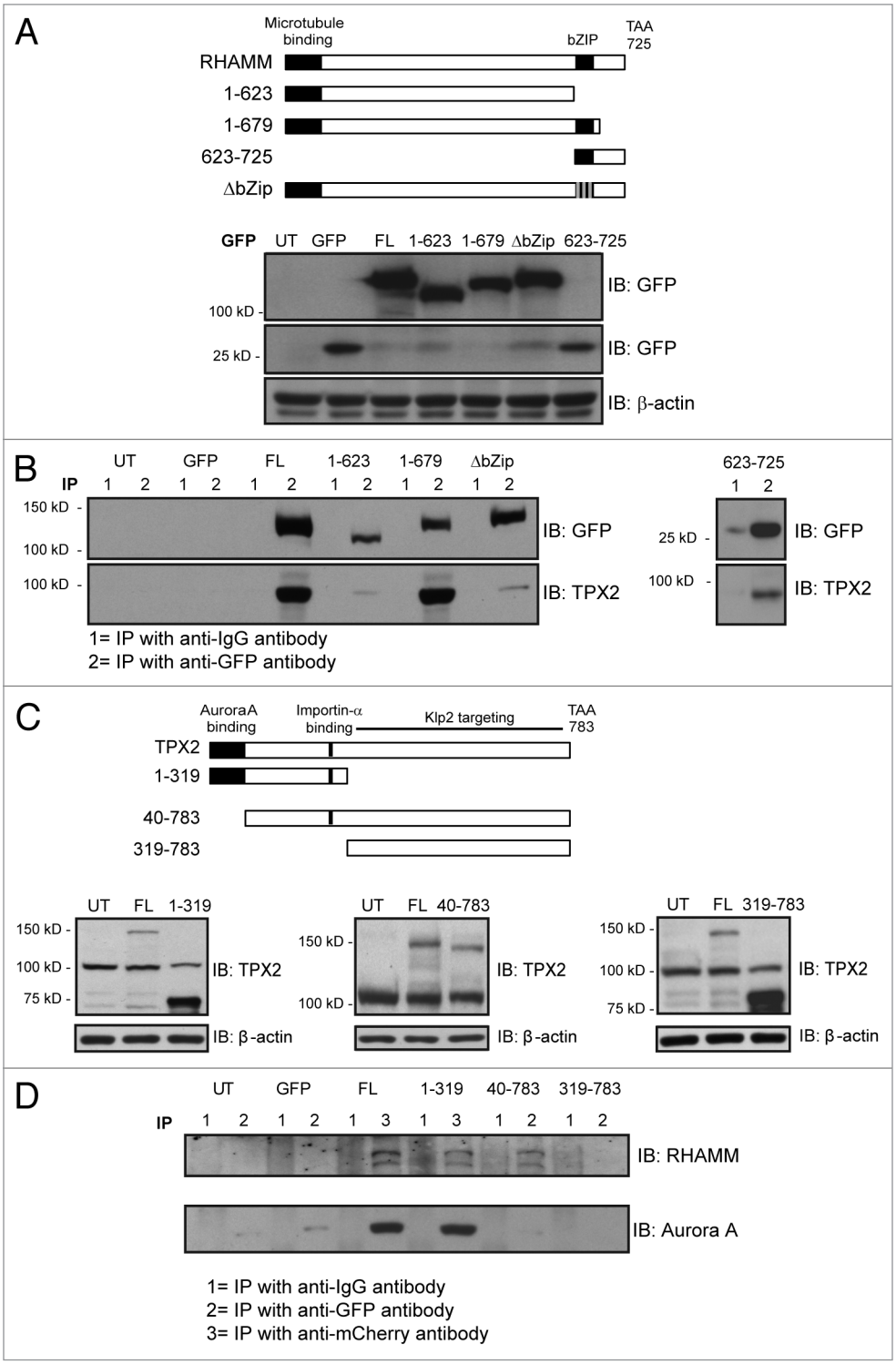

Figure 4. Characterization of the functional domains involved in RHAMM-TPX2 interaction during early mitosis. (**A**) Schematic diagram of defined domains in RHAMM. The 3 gray lines in the ΔbZIP construct represent leucines mutated to arginines. Western blot analysis confirmed the expression of GFP-RHAMM constructs. β-actin levels confirmed equal loading. (**B**) Immunoprecipitation of GFP-RHAMM constructs identified the bZIP motif as a necessary domain in RHAMM for the co-precipitation of TPX2. Cell lysates were immunoprecipitated with either an IgG control antibody (lanes marked 1) or antibodies against eGFP (lanes marked 2). (**C**) Schematic diagram of defined domains in TPX2. Western blot analysis confirmed the expression of mCherry-TPX2 and TPX2-GFP truncation variants. β-actin levels confirmed equal loading. (**D**) Immunoprecipitation of mCherry–TPX2 or TPX2–GFP truncation variants identified amino acids 40–319 as necessary for the co-precipitation of RHAMM. Cell lysates were immunoprecipitated with either an IgG control antibody (lane marked 1) or antibodies against eGFP (lane marked 2) or mCherry (lane marked 3).

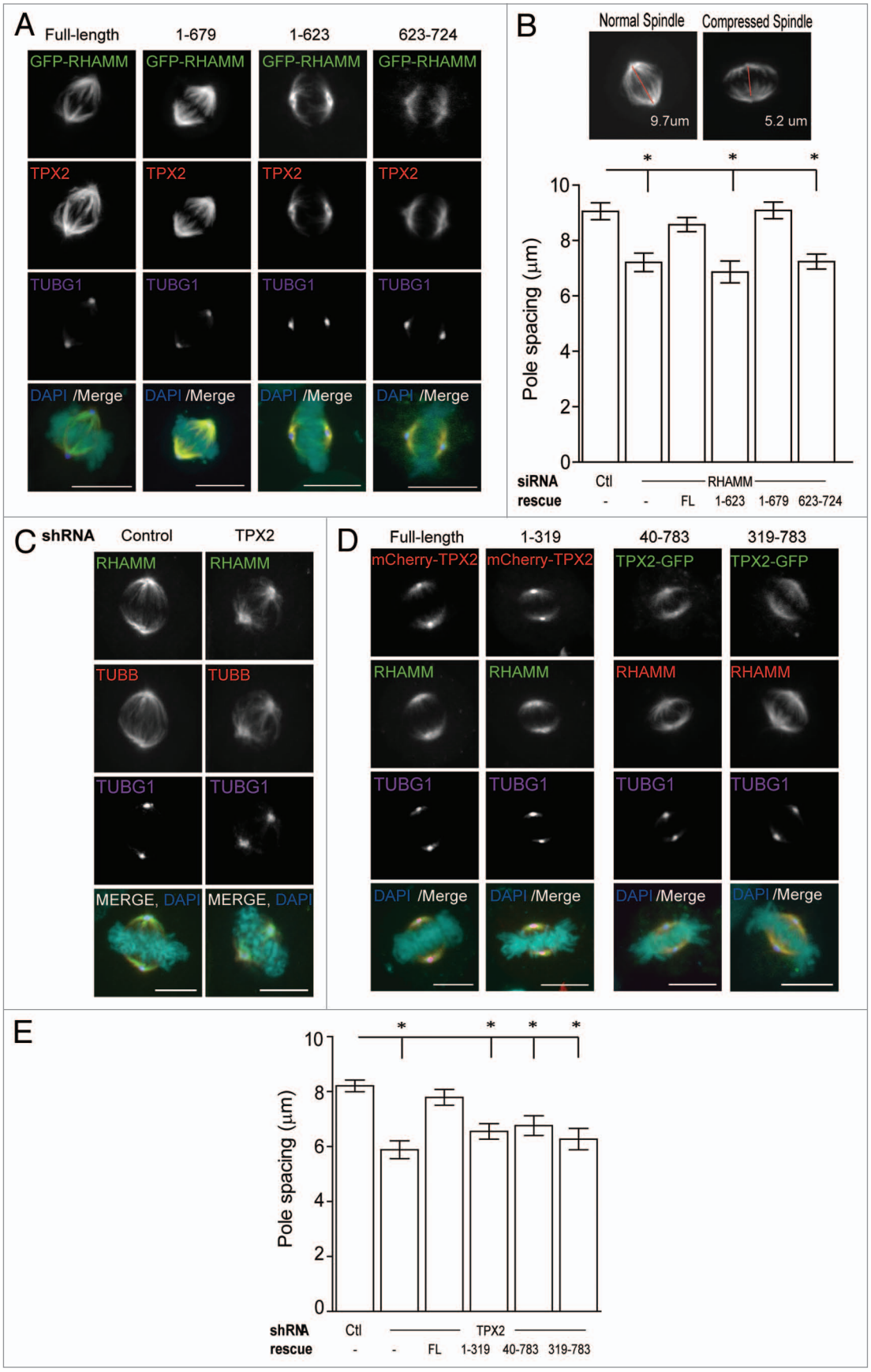

Figure 5. For figure legend, see page 2257.

Figure 5 (See previous page). Proper mitotic spindle length requires RHAMM targeting TPX2 to the spindle poles. (**A**) Cells treated with siRNA targeting RHAMM were transfected with the indicated GFP-RHAMM constructs, and asynchronous metaphase cells were analyzed by immunofluorescence. Amino acids 623–679 of RHAMM are the minimal required domain for protein localization to spindle poles (identified by TUBG1), while TPX2 localization to the spindle poles require additional residues. Scale bars = 10 μm. (**B**) Spindle length was measured based on TUBG1 staining in cells treated with either control siRNA or RHAMM targeted siRNA and followed by rescue with indicated GFP-RHAMM constructs. Measurements are made in a 3D projection along a plane perpendicular to the chromosomes. The bZIP motif (623–679) was necessary, though not sufficient, to establish proper mitotic spindle length. (mean ± SEM, n = 3, 30 cells per treatment, $^*P < 0.05$). (**C**) RHAMM remained localized at the spindle poles in cells treated with shRNA targeting TPX2. Scale bars = 10 μm. (**D**) Cells treated with shRNA targeting TPX2 were transfected with the indicated mCherry-TPX2 or TPX2-GFP constructs and asynchronous metaphase cells were analyzed by immunofluorescence. Scale bars = 10 μm. (**E**) Spindle length was measured based on TUBG1 staining in cells treated with either control shNHP or TPX2 targeted shRNA, and followed by rescue with indicated mCherry–TPX2 or TPX2–GFP constructs. Measurements are made in a 3D projection along a plane perpendicular to the chromosomes. (mean ± SEM, n = 1, >15 cells per treatment, $^*P < 0.05$).

other mitotic phenotypes identified by Neumann and colleagues revealed substantial overlap with defined kinetochore proteins, which suggests shared functions (**Fig. S1E**); phenotypes resulting from depletion of Aurora A, RHAMM, or TPX2 also overlap (**Fig. S1E**). Together, these results suggest that RHAMM influences mitotic events near to kinetochores, such as k-fiber assembly, chromosome attachment, and the successful completion of the spindle assembly checkpoint. Indeed, RHAMM, along with HURP, BARD1, and NuSAP, was targeted by the anaphase-promoting complex.[39] However, neither the correct localization of the BubR1 checkpoint protein nor the activation of the checkpoint in response to nocodazole were altered in published analyses of RHAMM-depleted cells.[9] Thus, a mechanistic role for RHAMM, if any, at kinetochores during the spindle assembly checkpoint is not currently clear.

RHAMM depletion prevented TPX2 localization at microtubule-assembly sites and augmented its proteasome-mediated proteolysis, which is likely prevented when TPX2 and Aurora A are in a complex.[26,40] Chemical inhibition of the proteasome rescued TPX2 and Aurora A abundance but incompletely recovered Aurora A activity in RHAMM-depleted cells. Thus, kinase activity required both abundance and the correct location of TPX2, and RHAMM was a necessary regulator for these 2 interdependent processes. Insufficient k-fiber assembly perturbs kinetochore-microtubule attachment, which affects spindle length due to a lack of resistance for poleward movement exerted by microtubule motors and downstream chromosome segregation. Consistently, RHAMM depletion reduced spindle length and gave rise to compressed spindles. However, k-fiber nucleation was not eliminated with RHAMM depletion, but rather was significantly attenuated and delayed to later time points in the microtubule-regrowth assay (**Video S7**). Thus, RHAMM was not essential for k-fiber assembly but enhanced this process by augmenting Aurora A activity at these sites.

While we showed here that RHAMM played a positive role in the correct location of TPX2 and the activation of Aurora A during spindle assembly, we do not discount that RHAMM, or a phosphorylated variant thereof, may also competitively inhibit the localization of TPX2. It is provocative, therefore, that we found the RHAMM-binding domain in TPX2 (aa 40–319) overlaps with the primary nuclear localization signal and an essential domain (aa 284–287) for an interaction with importin-α.[28] The proximity of these binding domains suggests that RHAMM may compete with importin-α for complexes with TPX2. If so, this may help to explain why the silencing of RHAMM altered the nuclear localization of TPX2 in interphase cells,[41] while the augmentation of RHAMM, through inhibition of BRCA1, mislocalized TPX2 during anastral assembly in *Xenopus* cells.[11] Moreover, the minimal interaction domain for RHAMM in TPX2 (aa 40–319) also contains a KEN box,[40] which is recognized by the anaphase promoting complex/cyclosome for targeted degradation and may help to explain how the silencing of RHAMM attenuates TPX2 stability. Taken together, our data identify RHAMM as a new and central regulator for Aurora A activity; modulation of RHAMM and its subsequent influence on TPX2 location and abundance may affect Aurora A kinase activity in a cell-type and context-dependent manner.[42,43]

Materials and Methods

Cell culture and cell cycle synchronization

HeLa cells were purchased from ATCC and cultured in Dulbecco modified Eagle medium (DMEM, Thermo-Fisher) supplemented with 10% fetal bovine serum (Invitrogen). HeLa cells that stably express eGFP-α-Tubulin and mCherry-Histone-H2B were kindly provided (Gruneberg Lab, University of Liverpool)[44] and maintained in media with 0.3 μg/ml puromycin (Invitrogen) and 0.5 μg/ml blasticidin S (Invitrogen). RPMI 8226 cells were purchased from ATCC and cultured in ATCC-formulated RPMI-1640 Medium (ATCC) supplemented with 10% fetal bovine serum (Invitrogen). All cell lines were grown at 37 °C in a 5% (v/v) CO_2 incubator. For synchronization, cells were subjected to a double thymidine block with 2 mM thymidine (Sigma) as described.[41]

Reagents and antibodies

Proteasome inhibitor MG132 (Sigma), MLN8237 (Selleck Chemicals), and BI2536 (Selleck Chemicals) were used as indicated. The following antibodies were used for immunoblotting and immunofluorescence: anti-Aurora A/AIK (Cell Signaling), anti-Phospho-Aurora A (Cell Signaling), anti-actin (Sigma), anti-BubR1 (Cell Signaling), anti-eGFP (Abcam), anti-GAPDH (Fitzgerald), anti-mCherry (Abcam), anti-RHAMM (Epitomics), anti-TPX2 (Novus Biologicals), anti-TUBG1 (Sigma Aldrich), anti-Ran (Cell Signaling), and anti-β-tubulin (Cell Signaling). Secondary antibodies were conjugated to IRDye (Rockland), HRP (Sigma), or to Alexa Fluor 488, 594, or 679 (Invitrogen). DAPI was purchased from Sigma Aldrich.

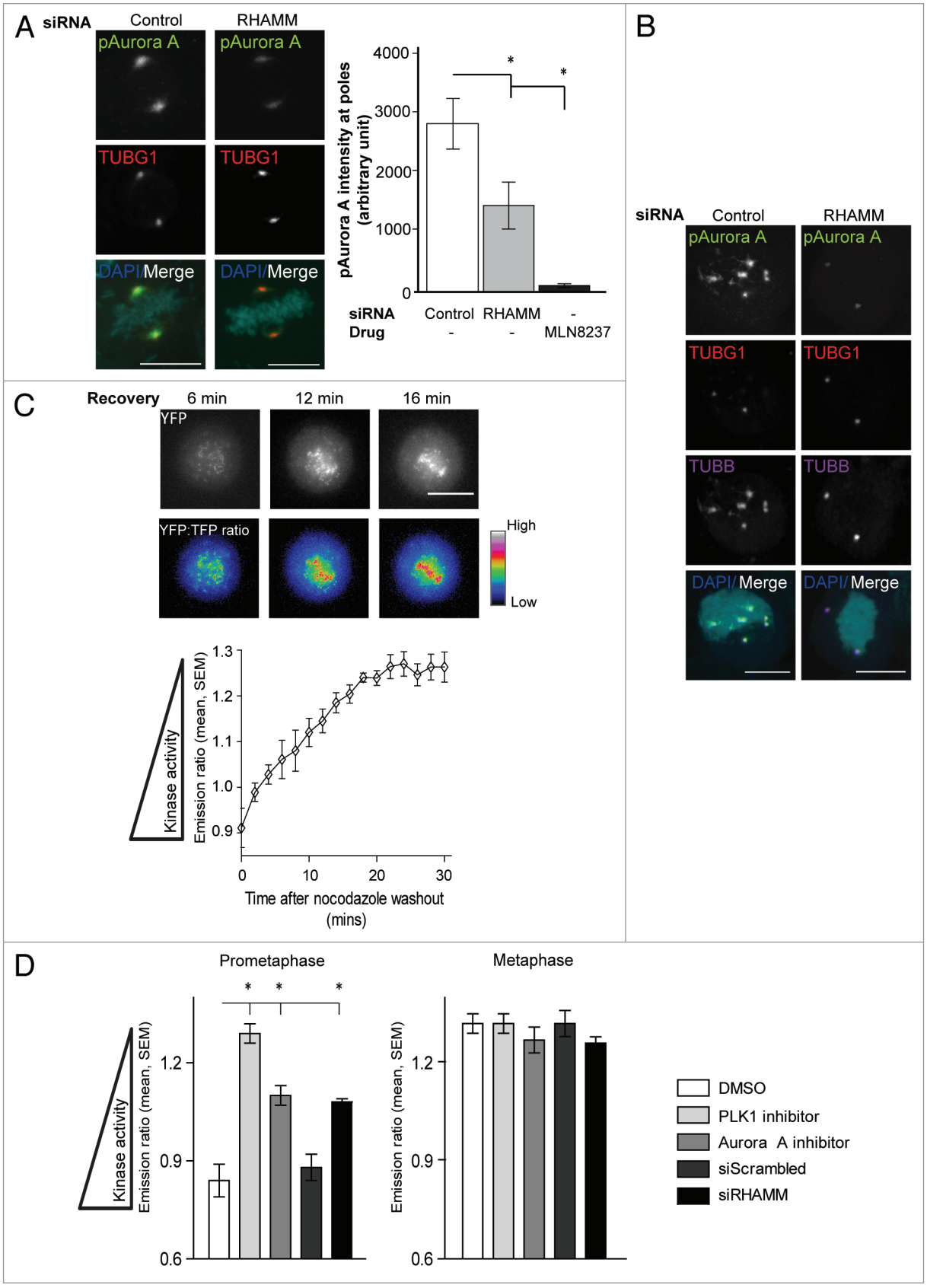

Figure 6. For figure legend, see page 2259.

Figure 6 (See previous page). RHAMM is required for the temporally- and spatially- regulated activity of Aurora A. (**A**) pAurora A specific immunoflourescence at the spindle poles (regions of interest identified by TUBG1) was significantly reduced in cells treated with MLN8237 (Aurora A specific inhibitor) or siRNA targeting RHAMM, relative to control siRNA-treated cells. Scale bars = 10 μm. (mean ± s.d., n = 3, *$P < 0.05$). (**B**) pAurora A localization to non-centrosome microtubule assembly sites was abolished in RHAMM-silenced mitotic cells during recovery from nocodazole treatment. Scale bars = 10 μm. (**C**) HeLa cells expressing a Hec-1 targeted PLK1 FRET sensor were imaged during recovery from nocodazole treatment. Phosphorylation of the kinetochore-targeted sensor was highest in early prometaphase (0–18 min) and diminished to background levels by metaphase (18–20 min) as indicated by the YFP:TFP emission ratio. Scale bars = 10 μm. (mean ± SEM., n = 3, 6 cells per treatment). (**D**) Relative to measurements in cells incubated with DMSO vehicle control, FRET ratios for the Hec-1 targeted PLK1 substrate were significantly higher in cells incubated with either a PLK1-specific inhibitor (BI2536, 20 nM for 2 h) or an Aurora A-specific inhibitor (MLN8237, 1 μM for 2 h) during prometaphase (2 min after nocodazole washout). Pretreatment of cells with siRNA targeting RHAMM, but not with scrambled siRNA controls, also significantly augmented the FRET emission ratio in prometaphase cells. No significant change in the FRET ratio was observed in metaphase cells (20 min after nocodazole washout) (mean ± SEM., n = 3, 6 cells per treatment, *$P < 0.05$).

Molecular cloning and site directed mutagenesis

Truncation variants of RHAMM and TPX2 were constructed using the Gateway cloning system by Invitrogen. DNA fragments of RHAMM(1–623), RHAMM(1–679), and RHAMM(623–725) were amplified from eGFPC1-RHAMM.[6] TPX2(1–319) was amplified from mCherry-TPX2 (Origene), while TPX2(40–783) and TPX2(319–783) were amplified from TPX2-GFP (Origene). Products were cloned into pDONR223 and transferred into pLenti6/V5-DEST or pDEST57 expression vectors (Invitrogen). Site-directed mutagenesis was performed using the QuikChange II kit (Agilent). Primer sequences used for PCR were listed in **Table S1**.

Transfection (siRNA and plasmids)

On-target plus siRNA (Dharmacon) sequences are listed in **Table S1**. Scrambled siRNA was used as a negative control. Transfections of siRNA and plasmid used Lipofectamine 2000™ (Invitrogen) following the manufacturer's protocols. Message and protein expression levels were measured 48–72 h post-transfection.

Lentivirus-mediated shRNA knockdown and generation of sub-lines

Lentivirus packaging, envelope, and control non-hairpin (NHP) pLKO.1 plasmids (Addgene) were used with shRNA against TPX2 (Sigma) as described[41] (**Table S1**). Transfected cells were selected with 0.5 μg/ml puromycin (GIBCO) for 1 wk and maintained with 0.3 μg/ml puromycin.

RT-PCR and qPCR

Total RNA was extracted from cells using RNeasy mini kit (Qiagen), quantified with NanoDrop (Thermo-Fisher), and 1 μg of total RNA was converted to cDNA using AccessQuick (VWR). qPCR reactions were run in triplicate in an 7000 series machine (Applied Biosystems). Analysis of qPCR results was done using the delta delta Ct method. Expression of RHAMM mRNA was normalized to the level of TATA box binding protein (TBP). Primers and conditions are listed in **Table S1**.

Western blot and immunoprecipitation

Cells were lysed at 0.5–1.0 × 10^7 cells/ml in RIPA buffer (western blot) or 0.5% NP-40 immunoprecipitation buffer (50 mM TRIS-HCl, pH 7.4, 150 mM NaCl, 1 mM EDTA, 0.5% NP-40) supplemented with protease inhibitors (Roche). Cell lysates were clarified by centrifugation at 16 000 × g for 10 min at 4 °C, and protein concentration was determined using the BCA protein assay kit (Pierce). For immunoprecipitation, lysates were precleared with protein A/G PLUS-Agarose beads (Santa Cruz) for 2 h at 4 °C with rotation. Protein complexes were isolated by incubation with 2.5 μg antibodies for 6 h at 4 °C with rotation, and then with protein A/G PLUS-Agarose beads for 4 h at 4 °C with rotation. Isolated complexes were washed 3 times with lysis buffer. Lysates were mixed with SDS sample buffer, separated by SDS-PAGE, and blotted with indicated primary antibodies and detected by HRP- or IRDye-conjugated antibodies and enhanced chemiluminescence (GE Healthcare) or Odyssey IR imaging (LI-COR) system, respectively.

Microtubule regrowth assay

Microtubules were depolymerized by treating cells with 5 μM nocodazole (Sigma) for 1 h at 37 °C. Cells were then washed 3 times with PBS and incubated in warm fresh media at 37 °C to allow microtubule regrowth. Cells were fixed at specified time points or living cells were imaged.

Immunofluorescence and image acquisition

Cells grown on coverslips were fixed with cold methanol. Cells were permeabilized with PBS-0.25% Triton X-100. Antibodies were diluted in PBS with 0.1% Triton X-100 and 3% BSA. Cells were washed 3 times in PBS-0.5% Tween-20 before and after incubations. Coverslips were mounted with ProLong Gold Antifade Reagent containing DAPI (Invitrogen).

Fixed cells were imaged using a 60× 1.2NA oil objective with the Fluoview software (Olympus) on the Olympus Fluoview FV10i (Olympus). Image stacks of 9 optical sections with a spacing of 1.0 μm through the cell volume were taken. Maximum intensity projection of the fluorescent channels was performed in ImageJ v1.46j (National Institute of Health).

For live-cell imaging, the glass coverslip was mounted in a silicone gasket (Chamlide CMM) and placed in a 37 °C and 5% CO_2 environmental chamber (Precision Control). Images were taken using a 40× 0.75 NA dry objective with the MetaMorph 7.5 software (Molecular Devices Inc) on the Olympus IX81 epifluorecent microscope (Olympus). For mitosis analysis, images were taken every 15 min using 350-ms exposures 2 × 2 binned resolution, with 2% of full lamp intensity per channel, and 7 optical sections spaced 1.0 μm apart. For microtubule regrowth analysis, images were taken every 2 min using 350-ms exposures 2 × 2 binned resolution, with 2% of full lamp intensity, and 7 optical sections spaced 1.0 μm apart. Maximum intensity projection of the fluorescent channels was performed in MetaMorph (Molecular Devices Inc).

Live imaging of the FRET (fluorescence resonance energy transfer) biosensor (kindly provided by the Lampson lab, University of Pennsylvania)[31] was performed using the Olympus IX81 epifluorescent microscope equipped with a 60× 1.35NA oil

objective, a cooled charge coupled device camera (CoolSNAP HQ2; Photometrics) controlled by the MetaMorph 7.5 software (Molecular Devices Inc). TFP and YFP emissions were acquired simultaneously with a 505DCXR beam splitter (Dual-View; Optical Insights, LLC) with the following optical filters: 438/24 for TFP excitation; 480/30 for TFP and 535/40 for YFP emission, respectively. Images were taken every 2 min using 300-ms exposures at 2 × 2 binned resolution for 30 min after nocodazole washout, with 45% of lamp intensity (X-Cite exacte, Lumen Dynamics) and 5 optical sections spaced 1.0 μm apart. Post-acquisition processing of images was performed using ImageJ v1.46j (National Institute of Health), as follows. The TFP and YFP emission images were background corrected by subtracting the value obtained from the cytoplasm, which does not include the kinetochore regions. The YFP/TFP FRET emission ratio value was then calculated as an average for the region of interest that was demarcated by the whole cell. Pseudocolored FRET images were generated by viewing the ratiometric data using the Ratio LUT (Look Up Table) plugin in ImageJ.

Statistics

Data were expressed as mean ± standard deviation for all figures except **Figure 3C and D**, which are mean ± standard error of mean. Statistical analysis was performed by unpaired 2-tailed Student *t* test. The results were considered significant at $P < 0.05$.

Disclosure of Potential Conflicts of Interest

No potential conflicts of interest were disclosed.

Author Contributions

H.C., P.M., O.N., D.H., and J.J. performed all experiments and data analysis. M.C.F., D.N., L.M.P., and C.J.L. provided reagents and expertise. C.A.M. designed the study, assisted in the analysis, and, along with H.C., wrote the manuscript.

Funding

These studies were supported by an operating grant from the Canadian Institutes of Health Research (CIHR), in partnership with the Avon Foundation for Women- Canada (Grant No. 201309OBC). H.C. was supported by a graduate studentship from the Child and Family Research Institute (CFRI). O.N. was supported by graduate studentships from the CFRI and a Banting and Best MSc studentship from CIHR.

Supplemental Materials

Supplemental materials may be found here:
www.landesbioscience.com/journals/cc/article/29270

References

1. Walczak CE, Cai S, Khodjakov A. Mechanisms of chromosome behaviour during mitosis. Nat Rev Mol Cell Biol 2010; 11:91-102; PMID:20068571
2. Barros TP, Kinoshita K, Hyman AA, Raff JW. Aurora A activates D-TACC-Msps complexes exclusively at centrosomes to stabilize centrosomal microtubules. J Cell Biol 2005; 170:1039-46; PMID:16186253; http://dx.doi.org/10.1083/jcb.200504097
3. Giet R, McLean D, Descamps S, Lee MJ, Raff JW, Prigent C, Glover DM. Drosophila Aurora A kinase is required to localize D-TACC to centrosomes and to regulate astral microtubules. J Cell Biol 2002; 156:437-51; PMID:11827981; http://dx.doi.org/10.1083/jcb.200108135
4. Terada Y, Uetake Y, Kuriyama R. Interaction of Aurora-A and centrosomin at the microtubule-nucleating site in Drosophila and mammalian cells. J Cell Biol 2003; 162:757-63; PMID:12939255; http://dx.doi.org/10.1083/jcb.200305048
5. Mori D, Yano Y, Toyo-oka K, Yoshida N, Yamada M, Muramatsu M, Zhang D, Saya H, Toyoshima YY, Kinoshita K, et al. NDEL1 phosphorylation by Aurora-A kinase is essential for centrosomal maturation, separation, and TACC3 recruitment. Mol Cell Biol 2007; 27:352-67; PMID:17060449; http://dx.doi.org/10.1128/MCB.00878-06
6. Maxwell CA, Keats JJ, Crainie M, Sun X, Yen T, Shibuya E, Hendzel M, Chan G, Pilarski LM. RHAMM is a centrosomal protein that interacts with dynein and maintains spindle pole stability. Mol Biol Cell 2003; 14:2262-76; PMID:12808028; http://dx.doi.org/10.1091/mbc.E02-07-0377
7. Maxwell CA, Keats JJ, Belch AR, Pilarski LM, Reiman T. Receptor for hyaluronan-mediated motility correlates with centrosome abnormalities in multiple myeloma and maintains mitotic integrity. Cancer Res 2005; 65:850-60; PMID:15705883
8. Tolg C, Hamilton SR, Morningstar L, Zhang J, Zhang S, Esguerra KV, Telmer PG, Luyt LG, Harrison R, McCarthy JB, et al. RHAMM promotes interphase microtubule instability and mitotic spindle integrity through MEK1/ERK1/2 activity. J Biol Chem 2010; 285:26461-74; PMID:20558733; http://dx.doi.org/10.1074/jbc.M110.121491
9. Dunsch AK, Hammond D, Lloyd J, Schermelleh L, Gruneberg U, Barr FA. Dynein light chain 1 and a spindle-associated adaptor promote dynein asymmetry and spindle orientation. J Cell Biol 2012; 198:1039-54; PMID:22965910; http://dx.doi.org/10.1083/jcb.201202112
10. Groen AC, Cameron LA, Coughlin M, Miyamoto DT, Mitchison TJ, Ohi R. XRHAMM functions in ran-dependent microtubule nucleation and pole formation during anastral spindle assembly. Curr Biol 2004; 14:1801-11; PMID:15498487; http://dx.doi.org/10.1016/j.cub.2004.10.002
11. Joukov V, Groen AC, Prokhorova T, Gerson R, White E, Rodriguez A, Walter JC, Livingston DM. The BRCA1/BARD1 heterodimer modulates ran-dependent mitotic spindle assembly. Cell 2006; 127:539-52; PMID:17081976; http://dx.doi.org/10.1016/j.cell.2006.08.053
12. Wittmann T, Boleti H, Antony C, Karsenti E, Vernos I. Localization of the kinesin-like protein Xklp2 to spindle poles requires a leucine zipper, a microtubule-associated protein, and dynein. J Cell Biol 1998; 143:673-85; PMID:9813089; http://dx.doi.org/10.1083/jcb.143.3.673
13. Bayliss R, Sardon T, Vernos I, Conti E. Structural basis of Aurora-A activation by TPX2 at the mitotic spindle. Mol Cell 2003; 12:851-62; PMID:14580337; http://dx.doi.org/10.1016/S1097-2765(03)00392-7
14. Dodson CA, Bayliss R. Activation of Aurora-A kinase by protein partner binding and phosphorylation are independent and synergistic. J Biol Chem 2012; 287:1150-7; PMID:22094468; http://dx.doi.org/10.1074/jbc.M111.312090
15. Pujana MA, Han JD, Starita LM, Stevens KN, Tewari M, Ahn JS, Rennert G, Moreno V, Kirchhoff T, Gold B, et al. Network modeling links breast cancer susceptibility and centrosome dysfunction. Nat Genet 2007; 39:1338-49; PMID:17922014; http://dx.doi.org/10.1038/ng.2007.2
16. Katayama H, Sasai K, Kloc M, Brinkley BR, Sen S. Aurora kinase-A regulates kinetochore/chromatin associated microtubule assembly in human cells. Cell Cycle 2008; 7:2691-704; PMID:18773538; http://dx.doi.org/10.4161/cc.7.17.6460
17. Booth DG, Hood FE, Prior IA, Royle SJA. A TACC3/ch-TOG/clathrin complex stabilises kinetochore fibres by inter-microtubule bridging. EMBO J 2011; 30:906-19; PMID:21297582; http://dx.doi.org/10.1038/emboj.2011.15
18. Sankaran S, Crone DE, Palazzo RE, Parvin JD. Aurora-A kinase regulates breast cancer associated gene 1 inhibition of centrosome-dependent microtubule nucleation. Cancer Res 2007; 67:11186-94; PMID:18056443; http://dx.doi.org/10.1158/0008-5472.CAN-07-2578
19. Sankaran S, Starita LM, Groen AC, Ko MJ, Parvin JD. Centrosomal microtubule nucleation activity is inhibited by BRCA1-dependent ubiquitination. Mol Cell Biol 2005; 25:8656-68; PMID:16166645; http://dx.doi.org/10.1128/MCB.25.19.8656-8668.2005
20. Katayama H, Zhou H, Li Q, Tatsuka M, Sen S. Interaction and feedback regulation between STK15/BTAK/Aurora-A kinase and protein phosphatase 1 through mitotic cell division cycle. J Biol Chem 2001; 276:46219-24; PMID:11551964; http://dx.doi.org/10.1074/jbc.M107540200
21. Hirota T, Kunitoku N, Sasayama T, Marumoto T, Zhang D, Nitta M, Hatakeyama K, Saya H. Aurora-A and an interacting activator, the LIM protein Ajuba, are required for mitotic commitment in human cells. Cell 2003; 114:585-98; PMID:13678582; http://dx.doi.org/10.1016/S0092-8674(03)00642-1

22. Hutterer A, Berdnik D, Wirtz-Peitz F, Zigman M, Schleiffer A, Knoblich JA. Mitotic activation of the kinase Aurora-A requires its binding partner Bora. Dev Cell 2006; 11:147-57; PMID:16890155; http://dx.doi.org/10.1016/j.devcel.2006.06.002
23. Eckerdt F, Pascreau G, Phistry M, Lewellyn AL, DePaoli-Roach AA, Maller JL. Phosphorylation of TPX2 by Plx1 enhances activation of Aurora A. Cell Cycle 2009; 8:2413-9; PMID:19556869; http://dx.doi.org/10.4161/cc.8.15.9086
24. Gruss OJ, Carazo-Salas RE, Schatz CA, Guarguaglini G, Kast J, Wilm M, Le Bot N, Vernos I, Karsenti E, Mattaj IW. Ran induces spindle assembly by reversing the inhibitory effect of importin alpha on TPX2 activity. Cell 2001; 104:83-93; PMID:11163242; http://dx.doi.org/10.1016/S0092-8674(01)00193-3
25. Kalab P, Heald R. The RanGTP gradient - a GPS for the mitotic spindle. J Cell Sci 2008; 121:1577-86; PMID:18469014; http://dx.doi.org/10.1242/jcs.005959
26. Giubettini M, Asteriti IA, Scrofani J, De Luca M, Lindon C, Lavia P, Guarguaglini G. Control of Aurora-A stability through interaction with TPX2. J Cell Sci 2011; 124:113-22; PMID:21147853; http://dx.doi.org/10.1242/jcs.075457
27. Brunet S, Sardon T, Zimmerman T, Wittmann T, Pepperkok R, Karsenti E, Vernos I. Characterization of the TPX2 domains involved in microtubule nucleation and spindle assembly in Xenopus egg extracts. Mol Biol Cell 2004; 15:5318-28; PMID:15385625; http://dx.doi.org/10.1091/mbc.E04-05-0385
28. Giesecke A, Stewart M. Novel binding of the mitotic regulator TPX2 (target protein for Xenopus kinesin-like protein 2) to importin-alpha. J Biol Chem 2010; 285:17628-35; PMID:20335181; http://dx.doi.org/10.1074/jbc.M110.102343
29. Bird AW, Hyman AA. Building a spindle of the correct length in human cells requires the interaction between TPX2 and Aurora A. J Cell Biol 2008; 182:289-300; PMID:18663142; http://dx.doi.org/10.1083/jcb.200802005
30. Greenan G, Brangwynne CP, Jaensch S, Gharakhani J, Jülicher F, Hyman AA. Centrosome size sets mitotic spindle length in Caenorhabditis elegans embryos. Curr Biol 2010; 20:353-8; PMID:20137951; http://dx.doi.org/10.1016/j.cub.2009.12.050
31. Liu D, Davydenko O, Lampson MA. Polo-like kinase-1 regulates kinetochore-microtubule dynamics and spindle checkpoint silencing. J Cell Biol 2012; 198:491-9; PMID:22908307; http://dx.doi.org/10.1083/jcb.201205090
32. Bruinsma W, Macurek L, Freire R, Lindqvist A, Medema RH. Bora and Aurora-A continue to activate Plk1 in mitosis. J Cell Sci 2014; 127:801-11; PMID:24338364; http://dx.doi.org/10.1242/jcs.137216
33. De Luca M, Lavia P, Guarguaglini G. A functional interplay between Aurora-A, Plk1 and TPX2 at spindle poles: Plk1 controls centrosomal localization of Aurora-A and TPX2 spindle association. Cell Cycle 2006; 5:296-303; PMID:16418575; http://dx.doi.org/10.4161/cc.5.3.2392
34. Macůrek L, Lindqvist A, Lim D, Lampson MA, Klompmaker R, Freire R, Clouin C, Taylor SS, Yaffe MB, Medema RH. Polo-like kinase-1 is activated by aurora A to promote checkpoint recovery. Nature 2008; 455:119-23; PMID:18615013; http://dx.doi.org/10.1038/nature07185
35. Archambault V, Carmena M. Polo-like kinase-activating kinases: Aurora A, Aurora B and what else? Cell Cycle 2012; 11:1490-5; PMID:22433949; http://dx.doi.org/10.4161/cc.19724
36. Neumann B, Walter T, Hériché JK, Bulkescher J, Erfle H, Conrad C, Rogers P, Poser I, Held M, Liebel U, et al. Phenotypic profiling of the human genome by time-lapse microscopy reveals cell division genes. Nature 2010; 464:721-7; PMID:20360735; http://dx.doi.org/10.1038/nature08869
37. Sharp JA, Plant JJ, Ohsumi TK, Borowsky M, Blower MD. Functional analysis of the microtubule-interacting transcriptome. Mol Biol Cell 2011; 22:4312-23; PMID:21937723; http://dx.doi.org/10.1091/mbc.E11-07-0629
38. Glover DM, Leibowitz MH, McLean DA, Parry H. Mutations in aurora prevent centrosome separation leading to the formation of monopolar spindles. Cell 1995; 81:95-105; PMID:7720077; http://dx.doi.org/10.1016/0092-8674(95)90374-7
39. Song L, Rape M. Regulated degradation of spindle assembly factors by the anaphase-promoting complex. Mol Cell 2010; 38:369-82; PMID:20471943; http://dx.doi.org/10.1016/j.molcel.2010.02.038
40. Stewart S, Fang G. Anaphase-promoting complex/cyclosome controls the stability of TPX2 during mitotic exit. Mol Cell Biol 2005; 25:10516-27; PMID:16287863; http://dx.doi.org/10.1128/MCB.25.23.10516-10527.2005
41. Maxwell CA, Benítez J, Gómez-Baldó L, Osorio A, Bonifaci N, Fernández-Ramires R, Costes SV, Guinó E, Chen H, Evans GJ, et al.; HEBON; EMBRACE; SWE-BRCA; BCFR; GEMO Study Collaborators; kConFab. Interplay between BRCA1 and RHAMM regulates epithelial apicobasal polarization and may influence risk of breast cancer. PLoS Biol 2011; 9:e1001199; PMID:22110403; http://dx.doi.org/10.1371/journal.pbio.1001199
42. Mohan P, Castellsague J, Jiang J, Allen K, Chen H, Nemirovsky O, Spyra M, Hu K, Kluwe L, Pujana MA, et al. Genomic imbalance of HMMR/RHAMM regulates the sensitivity and response of malignant peripheral nerve sheath tumour cells to aurora kinase inhibition. Oncotarget 2013; 4:80-93; PMID:23328114
43. Jiang J, Mohan P, Maxwell CA. The cytoskeletal protein RHAMM and ERK1/2 activity maintain the pluripotency of murine embryonic stem cells. PLoS One 2013; 8:e73548; PMID:24019927; http://dx.doi.org/10.1371/journal.pone.0073548
44. Zeng K, Bastos RN, Barr FA, Gruneberg U. Protein phosphatase 6 regulates mitotic spindle formation by controlling the T-loop phosphorylation state of Aurora A bound to its activator TPX2. J Cell Biol 2010; 191:1315-32; PMID:21187329; http://dx.doi.org/10.1083/jcb.201008106